

# Topological States and Adiabatic Pumping in Quasicrystals

Yaacov E. Kraus,<sup>1</sup> Yoav Lahini,<sup>2</sup> Zohar Ringel,<sup>1</sup> Mor Verbin,<sup>2</sup> and Oded Zilberberg<sup>1</sup>  
(Author names appear in alphabetic order.)

<sup>1</sup>*Department of Condensed Matter Physics, Weizmann Institute of Science, Rehovot, Israel.*  
<sup>2</sup>*Department of Physics of Complex Systems, Weizmann Institute of Science, Rehovot, Israel.*

The discovery of topological insulators<sup>1</sup> has sparked considerable interest in the study of topological phases of matter. The hallmark of these novel phases is the emergence of topologically protected boundary phenomena<sup>1</sup>, e.g. quantum pumping<sup>2,3</sup>, surface states related to exotic models from particle physics<sup>4</sup> and quasi-particles with non-Abelian statistics<sup>5</sup>. Yet, realizations of these phases of matter are scarce<sup>6–11</sup>. Additionally, one-dimensional systems without any additional symmetries are considered to lack such topological phenomena<sup>12</sup>. Here we show, both theoretically and experimentally, that quasicrystals possess high-dimensional topological phases. We demonstrate that one-dimensional quasicrystals exhibit topological properties that were, thus far, thought to be limited to two-dimensional systems. Using photonic quasicrystals, we observe localized boundary states, which manifest these topological properties. These topological boundary states are used to realize an adiabatic optical pumping effect in which photons are unidirectionally pumped across the sample. Generalization to various types of quasicrystals and higher dimensions are also discussed, suggesting the existence of topological effects on surfaces of three-dimensional quasicrystals. This work opens a path to the realization of new types of topological phases, and provides new insights to the physics of quasicrystals.

Topological phases of matter consist of various band insulators or superconductors that have gaps in their spectrum<sup>1</sup>. Two systems belong to the same topological phase if they can be continuously deformed from one into the other without closing energy gaps. Consequently, at the interface between two topologically distinct systems the energy gaps close by the appearance of boundary states which are localized on the interface. Classification of all the possible topological phases according to their symmetries and dimensionality was recently introduced<sup>13</sup>. For example, in the absence of any symmetries, all the one-dimensional (1D) systems belong to the topologically trivial phase, while in two-dimensions (2D) there is a well known series of topological phases, namely those of the Integer Quantum Hall Effect (IQHE)<sup>12</sup>.

Quasicrystals (QCs) are non-periodic structures that possess long-range order<sup>14</sup>. This quasi-periodic order can be seen as originating from periodic structures of a dimension higher than the physical one. For example, the 1D Fibonacci QC can be described as a projection of a

2D lattice on a line<sup>14</sup>. Remarkably, observed phenomena such as unconventional Bragg diffraction and the existence of Phasons<sup>14–16</sup> can be attributed to this higher dimension. Indeed, remnants of the higher dimensionality appear as additional degrees of freedom (d.o.f.) in the form of shifts of the origin points of the quasi-periodic order. These d.o.f. discern between QCs with the same quasi-periodic order as they result in different patterns. However, they have no apparent influence on the bulk properties, and were therefore usually ignored.

In this work we show that due to these additional d.o.f., QCs exhibit non-trivial topological properties that are usually attributed to systems of a higher dimension. The topological properties of the QC manifest in two ways: (i) The existence of quantum phase transitions when transforming between two topologically distinct QCs; (ii) The appearance of robust boundary states which transverse the bulk gaps as a function of the aforementioned shifts. We demonstrate experimentally that 1D photonic QCs exhibit such boundary states. Harnessing the topological nature of these boundary states, we generate a quantum pump in which photons are transferred across the QC by shifting the pattern's origin adiabatically.

Let us begin with a specific example of a QC, the 1D Aubry-Andre (AA) model<sup>17</sup>. This is a 1D tight-binding model in which the on-site potential is modulated in space. It is described by the Hamiltonian

$$H(\phi)\psi_n = t(\psi_{n+1} + \psi_{n-1}) + \Lambda \cos(2\pi bn + \phi) \psi_n. \quad (1)$$

Here,  $\psi_n$  is the wavefunction at site  $n$ ,  $t$  is the hopping amplitude,  $\Lambda$  is the modulation amplitude of the on-site potential, and  $b$  controls the periodicity of the modulation. Whenever  $b$  is irrational the modulation is incommensurate with the lattice and the on-site term is quasi-periodic. Note that this model embeds the d.o.f. mentioned above in the form of the phase  $\phi$  of the spatial modulation.

Fig. 1a depicts the numerically calculated spectrum of the AA model as a function of  $\phi$  for  $t = 1$ ,  $\Lambda = 0.5$ ,  $b = (\sqrt{5} + 1)/2$  (the Golden mean) and  $n = -49..49$ . Due to the incommensurate potential, the spectrum is broken into a fractal set of bands and gaps<sup>17,18</sup>. Note that as a function of  $\phi$  the bands are almost unchanged, yet the gaps are crossed by a few modes. The states that reside within the gaps are boundary states, localized either on the left or on the right boundary of the system, as seen in insets (1) and (2), respectively, while the states within the bands are typically extended, as depicted in

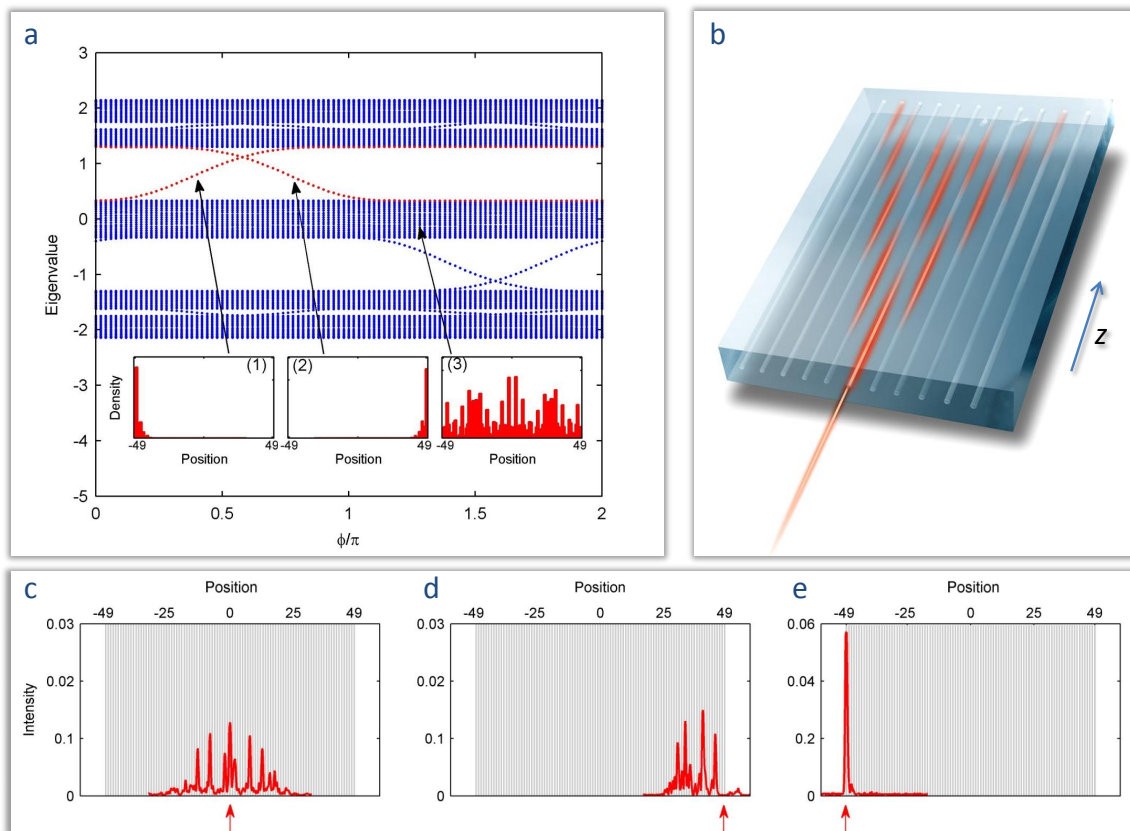


FIG. 1: Observation of topological boundary states in an Aubry-Andre photonic quasicrystal. (a) The numerically calculated spectrum (marked by blue and red dots) of equation (1) as a function of the phase  $\phi$  for  $t = 1$ ,  $\Lambda = 0.5$ ,  $b = (\sqrt{5} + 1)/2$ , and  $n = -49 \dots 49$ . The bulk of the spectrum remains fixed, whereas few modes, localized at the boundaries, sweep across the gaps. The insets depict the spatial density of typical eigenstates as a function of position along the 1D lattice: (1) a left boundary state; (2) a right boundary state; and (3) an extended state within the bands. (b) An illustration of the experimental system – the photonic waveguide lattice. Light that is injected into one of the waveguides tunnels to neighboring waveguides as it propagates. The propagation is described by equation (1) where the propagation axis,  $z$ , takes over the role of time. (c)-(e) Experimental observation of the left boundary state for  $\phi = \pi/2$ . Light was initially injected to a single waveguide (marked by red arrows). The measured outgoing intensity is plotted versus the position along the lattice. (c) An excitation at the middle of the lattice (site 0) results in a significant spread. (d) When the light was injected to the rightmost site (site 49), the excitation again shows comparable spread. (e) For an excitation at the leftmost site (site  $-49$ ), the light remains tightly localized at the boundary, marking the existence of a boundary state.

inset (3). As we later show, these boundary states are the physical manifestation of the fact that the AA model belongs to a non-trivial topological phase.

We implemented the AA model in an optical setup using a quasi-periodic array of coupled waveguides<sup>19</sup>, as illustrated in Fig. 1b (see Methods). In such systems light is injected into one of the waveguides, and is coherently coupled to neighboring waveguides as it propagates. The propagation of the light is described by an equation which is identical to a tight-binding model, where the propagation axis takes over the role of time<sup>20</sup>. By modulating the refraction index of the waveguides it is possible to directly realize the AA Hamiltonian of equation (1).

We fabricated an AA lattice with the above mentioned parameters and  $\phi = \pi/2$ . The experimental observations are depicted in Fig. 1c-e. When the light was injected

into a lattice site in the middle of the array, the outgoing intensity distribution showed a significant expansion, due to the overlap of the injected wavefunction with the extended bulk eigenstates. When light was injected into the rightmost lattice site it again showed considerable expansion, meaning that here too, the initial excitation overlapped mostly with extended bulk states. However, when the light was injected to the leftmost lattice site, the intensity distribution remained tightly localized at the boundary, with the maximum intensity found at the leftmost waveguide itself. This is a clear signature of the existence of a topological localized boundary state.

A consequence of the topological nature of this model is that all boundary states which reside within the same gap belong to the same mode. This can be seen by following the eigenenergy of some boundary state as a function of

$\phi$ . For example, take the right boundary state denoted in inset (2) of Fig. 1a. Its mode is marked by red circles. This state remains localized on the right boundary as long as its energy remains within the gap. When the energy reaches the band, the state becomes extended. Notably, once the mode returns into the gap it appears localized at the left boundary.

This property was used to realize adiabatic pumping of photons from one side of the lattice to the other. A convenient platform for this feat is the “off-diagonal” version of the AA model which is described by the Hamiltonian

$$H_{\text{off}}(\phi)\psi_n = t[1 + \Lambda \cos(2\pi bn + \phi)]\psi_{n+1} + t[1 + \Lambda \cos(2\pi b(n-1) + \phi)]\psi_{n-1}. \quad (2)$$

While this model embeds its quasi-periodicity in the hopping term, it has similar topological characteristics as its previously discussed “diagonal” version [cf. equation (1)]. The pumping takes place when  $\phi$  is adiabatically swept along the propagation axis  $z$ . This is achieved by slowly modifying the spacing between the waveguides along the propagation axis, as illustrated in Fig. 2a. In our implementation we chose  $t = 30/78$ ,  $\Lambda = 0.6$ ,  $b = (\sqrt{5} + 1)/2$ , and  $n = 1 \dots 21$ , and the length of the sample to be 75mm, which are 19.5 tunneling lengths. Fig. 2b depicts the spectrum of the system for these parameters as a function of  $\phi$ . The pumping from the right boundary to the left one was carried out by sweeping  $\phi$  from  $0.4\pi$  to  $1.6\pi$ . In order to observe different stages of the pumping process, we fabricated a set of 50 samples for which the light was allowed to propagate shorter distances within the modulation. Correspondingly, in the  $i^{\text{th}}$  sample  $\phi$  is modulated from  $0.4\pi$  to  $(0.4 + 1.2 \cdot i/50)\pi$ . For each sample, light was injected to the rightmost site and the output intensity distribution was measured. The collected results are summarized in Fig. 2c. The obtained intensity distributions are stacked incrementally according to their propagation distance, i.e. their final  $\phi$ . Thus, we reconstruct the light’s trajectory along the full adiabatic process. It is evident that the injected light was pumped adiabatically across the QC from one boundary to the other<sup>21</sup>.

We now turn to establish our results theoretically. We start by showing that the observed boundary states are of topological origin by mapping the AA model to the lattice version of the 2D IQHE<sup>22</sup>. In the latter, electrons hop on a 2D square lattice with lattice spacing  $a$  in the presence of a perpendicular magnetic field, with  $b$  flux quanta threading each square. Assuming one coordinate to be periodic, the system can be described by the Hamiltonian<sup>23</sup>  $\mathcal{H}\psi_{n,k} = \sum_k [t(\psi_{n+1,k} + \psi_{n-1,k}) + 2t \cos(2\pi bn + ka)\psi_{n,k}]$ , where  $k$  is the momentum along the periodic coordinate and  $n$  is the location in real space along the second coordinate. The energy spectrum of  $\mathcal{H}$  is gapped, and each gap is associated with a quantized Hall conductance  $\sigma_H = \nu e^2/h$ , with  $\nu$  an integer<sup>22</sup> known as the Chern number<sup>12</sup>. The inclusion of disorder and distortions in the Hamiltonian does not alter  $\sigma_H$  as long as the corresponding gap is maintained open<sup>24,25</sup>. Due to the fact that the energy

gap must be closed in order for  $\sigma_H$  to change its value, it can be used to classify different phases of the IQHE. Phases with different  $\sigma_H$  are said to be topologically distinct.

The physical manifestation of a non-trivial topological phase (i.e.  $\sigma_H \neq 0$ ) is the emergence of robust chiral states along the edges of the sample. This general phenomena is shared by many topological phases, not only the IQHE<sup>26-28</sup>. In the IQHE, on each edge exactly  $|\nu|$  edge states appear, and the energy of each edge state transverses the gap as  $k$  varies from  $-\pi/a$  to  $\pi/a$ . The signs of the group velocity of these edge states are opposite on opposite edges.

Turning back to the 1D AA model [cf. equation (1)], we shall now observe that it inherits its robust boundary states from the 2D IQHE. For  $\Lambda = 2t$  the spectrum of  $H(\phi)$  can be viewed as the  $k^{\text{th}}$  component of  $\mathcal{H}$  at  $k = \phi/a$ . Therefore, by scanning  $\phi$  from  $-\pi$  to  $\pi$ , the spectrum of  $H(\phi)$  reconstructs that of  $\mathcal{H}$ . Consequently, the chiral edge states that transverse the gaps as a function of  $k$  appear now as 1D boundary states that transverse the gaps with  $\phi$ . Since these boundary states are of topological origin, the only way to eliminate them is to close the energy gap that they transverse. In particular, disorder that does not close an energy gap does not eliminate the corresponding boundary states. For  $\Lambda \neq 2$ , a similar mapping exists to the IQHE on a rectangular lattice, which has similar topological behavior.

Note that the topology guarantees the existence of boundary states only for intervals of  $\phi$ . Hence, it does not guarantee that for any QC pattern they indeed appear. This can be seen, for example, in Fig. 2b where for  $\phi = 0$  one finds states localized on both boundaries, and for  $\phi = \pi$  there are none. Additionally, changing the number of lattice sites or translating them (e.g. taking  $n = 5 \dots 25$  instead of  $n = 1 \dots 21$ ), may alter dramatically the intervals of  $\phi$  for which boundary states appear.

So far, in order to witness the topological nature of the AA model we had to scan  $\phi$ . Ostensibly, one can associate a Chern number only to the union of all the  $H(\phi)$  Hamiltonians. However, we claim that it is possible to associate a Chern number to any  $H(\phi)$ . Intuitively, this is due to the fact that  $\phi$  is analogous to the Aharonov-Bohm flux in the IQHE<sup>24</sup>. Formally, one has to distinguish between the Hall conductance (Chern density) and the flux-averaged Hall conductance (Chern number), where only the latter is quantized. However, in actual experiments of the IQHE one measures the former, and yet a quantized conductance is obtained. This is due to the fact that in the IQHE the Hall conductance is constant for all values of the Aharonov-Bohm flux<sup>24,28</sup>. We argue that  $\phi$  exhibits a similar behavior, namely it does not change bulk properties such as the spectrum or the conductance.

The proof that the Chern density of the AA model is the same for all  $\phi$ ’s, and its generalizations to other QCs and topological indices, appears in the Supplementary material. Here we show that the bulk spectrum

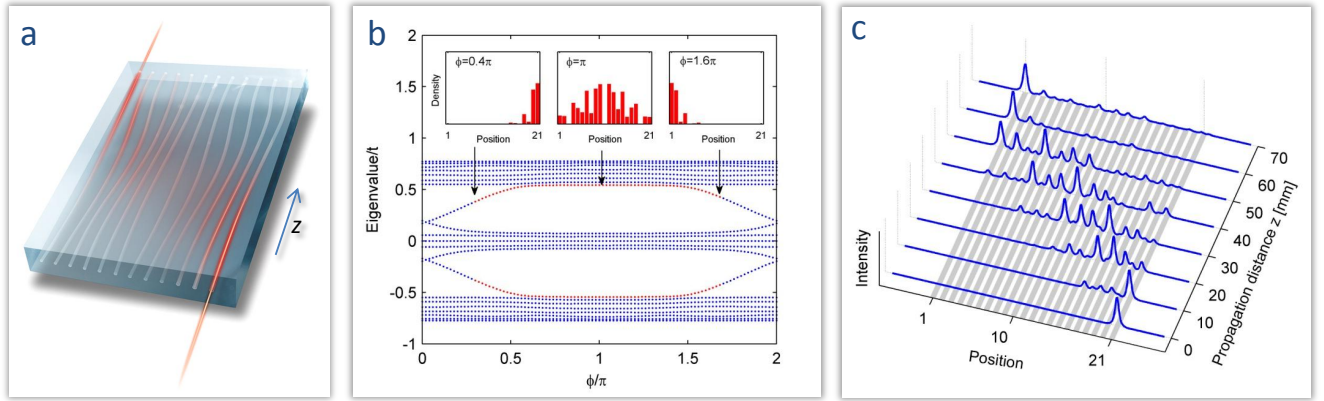


FIG. 2: Experimental observation of adiabatic pumping via topologically protected boundary states in a photonic quasicrystal. Here, we use the “off-diagonal” version of the Aubry-Andre model [see equation (2)] where the quasi-periodicity is in the hopping term. (a) An illustration of the adiabatically modulated photonic quasicrystal, constructed by slowly varying the spacing between the waveguides along the propagation axis  $z$ . Consequently, the injected light experiences an adiabatically modulated Hamiltonian,  $H_{\text{off}}(\phi(z))$ , as it propagates and is pumped across the sample. (b) The spectrum (marked by blue and red dots) of the model as a function of the phase  $\phi$  for  $t = 30/78$ ,  $\Lambda = 0.6$ ,  $b = (\sqrt{5} + 1)/2$ , and  $n = 1 \dots 21$ . In the experiment  $\phi$  was scanned between  $0.4\pi$  and  $1.6\pi$  as marked by the red dots. The insets depict the spatial density of a boundary eigenstate as function of the position at three different stages of the evolution: at  $\phi = 0.4\pi$  the eigenstate is localized on the right boundary of the lattice. At  $\phi = \pi$  it is delocalized across the system, while at  $\phi = 1.6\pi$  the state is again localized, but on the left boundary of the sample. (c) Experimental results: Light was injected to the rightmost waveguide (site 21) at  $z = 0$  ( $\phi = 0.4\pi$ ). The measured intensity distributions as a function of the position are presented at different stages of the adiabatic evolution, i.e. different propagation distances. It is evident that along the adiabatic evolution the light crossed the lattice from right to left.

is also independent of  $\phi$ . This simpler proof contains the essential ingredients of the former. Since  $H(\phi)$  has a band structure, the spectrum is insensitive to lattice translations in the thermodynamic limit. From equation (1) it is evident that translating the lattice by  $m$  sites is equivalent to shifting  $\phi$  by  $2\pi \cdot (bm \bmod 1)$ . Now the irrationality of  $b$  comes into play. For a rational  $b = p/q$ ,  $(bm \bmod 1)$  has only  $q$  different values for all possible translations. Thus, the band structure is guaranteed to be invariant only for these  $q$  corresponding shifts of  $\phi$ . On the other hand, for irrational  $b$ ,  $(bm \bmod 1)$  forms a dense set and the bands are invariant for any shift of  $\phi$ .

Thus we arrive at the following conclusion: while in order to witness boundary effects the scanning over  $\phi$  is required, the topological indices can be associated with any instance of a quasi-periodic pattern, i.e. any given  $\phi$ . These indices are, of course, the same for a given quasi-periodicity for all  $\phi$ 's. Thus the AA model is topologically classified. Consequently, two QCs with two different  $b$ 's cannot be smoothly deformed from one to the other without closing the bulk gaps, since in the IQHE different  $b$ 's result in different Chern numbers<sup>22</sup>.

Until now, we focused on a specific model which we were able to map to the IQHE. However, our results could be easily generalized to any QC<sup>29</sup> of any dimension and any topological classification without the need for establishing such a mapping. Consider a  $D$ -dimensional QC with a tight-binding Hamiltonian with  $d$  quasi-periodic terms, either hopping or on-site. These terms result in  $d$

d.o.f. similar to the above  $\phi$ . In the context of topological properties, these d.o.f. could be treated as extra dimensions, yielding an overall effective dimension of  $D + d$ . Therefore the Hamiltonian may belong to a non-trivial  $D + d$ -dimensional topological class. In such a case, the boundaries of the physical QC host boundary states for intervals of the d.o.f. and a quantum phase transition takes place when deforming between QCs with different topological indices.

In conclusion, we show that quasicrystals exhibit new types of topological phases, that were previously attributed only to systems of higher dimension. We demonstrate experimentally such topological effects in 1D systems using photonic quasicrystals. Moreover, we harness the topological nature of these 1D quasicrystals to realize an adiabatic pumping effect, observed directly in the optical setup. The study of the novel topological phases in 2D and 3D may lead to the discovery of new surface phenomena in atomic and photonic quasicrystals, e.g. 3D quasicrystalline materials may exhibit topological properties that would have appeared only in 6D periodic systems. Furthermore, our approach provides new tools for engineering photonic quasicrystals, and especially for controlling their surface properties.

## Methods

The first set of experiments was conducted using an array of evanescently coupled waveguides fabricated on a

semiconductor (ALGaAs) substrate using standard photolithography methods. In order to realize the AA model Hamiltonian [cf. equation (1)], we introduced a quasi-periodic modulation of the effective refraction index of the waveguides while keeping the period constant. The average width of the waveguides was  $3\mu\text{m}$ , and the period was  $9\mu\text{m}$ . The sample length was 20mm, which is equivalent to 30 tunneling lengths. The light source was a continuous-wave laser diode with a wavelength of 1550nm. The laser beam was focused into a single waveguide at the input facet of the array using a  $\times 40$  microscope objective. The light at the output facet was imaged

onto an infrared camera (Hamamatsu IR C5840).

For the adiabatic pumping experiments we used several arrays of waveguides written in bulk glass using femtosecond laser microfabrication technology. The waveguides were all identical in both refraction index and width ( $\sim 2\mu\text{m}$ ), while the inter-waveguide separation was modulated in order to realize the “off-diagonal” AA model [cf. equation (2)]. The sample length was 75mm, which is equivalent to 50 tunneling lengths. The number of waveguides in each array was 21. The light source was a continuous-wave laser diode with a wavelength of 808nm.

- 
- <sup>1</sup> M. Z. Hasan and C. L. Kane, *Rev. Mod. Phys.* **82**, 3045 (2010).
- <sup>2</sup> R. B. Laughlin, *Phys. Rev. B* **23**, 5632 (1981).
- <sup>3</sup> B. A. Bernevig and S. C. Zhang, *Phys. Rev. Lett.* **96**, 106802 (2006).
- <sup>4</sup> X.-L. Qi, T. L. Hughes, and S.-C. Zhang, *Phys. Rev. B* **78**, 195424 (2008).
- <sup>5</sup> C. Nayak, S. H. Simon, A. Stern, M. Freedman, and S. Das Sarma, *Rev. Mod. Phys.* **80**, 1083 (2008).
- <sup>6</sup> Y. Xia, D. Qian, D. Hsieh, L. Wray, A. Pal, H. Lin, Bansil, D. A. Grauer, Y. S. Hor, R. J. Cava, et al., *Nature Phys.* **5**, 398 (2009).
- <sup>7</sup> H. Zhang, C. X. Liu, X. L. Qi, X. Dai, Z. Fang, and S. C. Zhang, *Nature Phys.* **5**, 438 (2009).
- <sup>8</sup> S. Chadov, X. Qi, J. Kübler, G. H. Fecher, C. Felser, and S. C. Zhang, *Nature Mater.* **9**, 541 (2010).
- <sup>9</sup> H. Lin, L. A. Wray, Y. Xia, S. Xu, S. Jia, R. J. Cava, A. Bansil, and M. Z. Hasan, *Nature Mater.* **9**, 546 (2010).
- <sup>10</sup> M. Hafezi, E. A. Demler, M. D. Lukin, and J. M. Taylor, *Nature Phys.* (2011).
- <sup>11</sup> T. Kitagawa, M. S. Rudner, E. Berg, and E. Demler, *Phys. Rev. A* **82**, 033429 (2010), URL <http://link.aps.org/doi/10.1103/PhysRevA.82.033429>.
- <sup>12</sup> A. Y., R. Seiler, and S. B., *Nucl. Phys. B* **265**, 364 (1986).
- <sup>13</sup> S. Ryu, A. P. Schnyder, A. Furusaki, and A. W. W. Ludwig, *New Journal of Physics* **12**, 065010 (2010).
- <sup>14</sup> C. Janot, *Quasicrystals* (Clarendon, Oxford, 1994), 2nd ed.
- <sup>15</sup> J. E. S. Socolar, T. C. Lubensky, and P. J. Steinhardt, *Phys. Rev. B* **34**, 3345 (1986).
- <sup>16</sup> B. Freedman, G. Bartal, M. Segev, R. Lifshitz, D. N. Christodoulides, and J. W. Fleischer, *Nature* **440**, 1166 (2006).
- <sup>17</sup> S. Aubry and G. Andre, *Ann. Isr. Phys. Soc.* **3**, 133 (1980).
- <sup>18</sup> C. Aulbach, A. Wobst, G.-L. Ingold, P. Hänggi, and I. Varga, *New J. Phys.* **6**, 70 (2004).
- <sup>19</sup> Y. Lahini, R. Pugatch, F. Pozzi, M. Sorel, R. Morandotti, N. Davidson, and Y. Silberberg, *Phys. Rev. Lett.* **103**, 013901 (2009).
- <sup>20</sup> D. N. Christodoulides, F. Lederer, and Y. Silberberg, *Nature* **424**, 817 (2003).
- <sup>21</sup> This is analogous to Laughlin’s pumping in the IQHE<sup>2</sup>. However, here a single mode is being pumped, while in the IQHE all the electrons of the occupied band contribute to the current and induce the charge pumping.
- <sup>22</sup> D. R. Hofstadter, *Phys. Rev. B* **14**, 2239 (1976).
- <sup>23</sup> This Hamiltonian can be obtained by using the Pierels substitution in the hopping term, choosing the Landau gauge along the periodic coordinate and then Fourier transforming along this coordinate.
- <sup>24</sup> D. J. Thouless, M. Kohmoto, M. P. Nightingale, and M. den Nijs, *Phys. Rev. Lett.* **49**, 405 (1982).
- <sup>25</sup> D. Osadchy and J. E. Avron, *Journal of Mathematical Physics* **42**, 5665 (2001).
- <sup>26</sup> Y. Hatsugai, *Phys. Rev. Lett.* **71**, 3697 (1993).
- <sup>27</sup> C. L. Kane and E. J. Mele, *Phys. Rev. Lett.* **95**, 146802 (2005).
- <sup>28</sup> Z. Ringel and Y. E. Kraus, *Phys. Rev. B* **83**, 245115 (2011).
- <sup>29</sup> QCs obtained by a “cut and project” method also fit into our general argument, as shown in the Supplementary Material.

**Acknowledgments** We thank Y. Silberberg, S. Huber, R. Lifshits, Y. Gefen, and E. Altman for useful discussions; and N. Gontmakher for the illustration of the device. We especially thank Y. Silberberg for allowing us to conduct the experiments in his labs. Y.E.K. thanks the US-Israel Binational Science Foundation, and the Minerva foundation; Y.L. thanks the Israeli academy of science and humanities through the Adams program, and the Crown Photonics Center; Z.R. thanks the ISF grant 700822030182; M.V. thanks the Crown Photonics Center; O.Z. thanks the IMOS Israel-Korea grant and the Minerva foundation for financial support.

**Author Contributions** Y.E.K., Z.R. and O.Z. are responsible the theoretical part. Y.L. and M.V. designed and conducted the experiments. All authors contributed equally to this work.

## SUPPLEMENTARY MATERIAL

### I. THE CHERN NUMBER OF A QUASICRYSTAL

In this section we show that Chern numbers can be defined for any given 1D quasicrystal (QC). This is accomplished by proving that the Chern density associated with a gap of the QC is independent of the phase of the quasi-periodicity in the thermodynamic limit. The proof is presented for the Aubry-Andre (AA) model [cf. equation (1)], but can easily be generalized to other QCs and topological indices.

In order to evaluate the Chern number we consider a modified AA model with a similar spectrum. This model describes a periodic 1D lattice (a ring) of length  $L$  with an on-site potential parameterized by an irrational number  $b$ , and the Hamiltonian

$$H_b(\phi, \theta)\psi_n = te^{i\theta/L}\psi_{n+1} + te^{-i\theta/L}\psi_{n-1} + \Lambda \cos(2\pi\bar{b}_L n + \phi)\psi_n, \quad (3)$$

where  $\bar{b}_L = L[b/L]$ . It is clear that for  $\theta = 0$  and  $L \rightarrow \infty$  this Hamiltonian coincides with the one of the AA model. For finite but large  $L$ , the spectrum of  $H_b$  has the same gaps as those of the AA model, up to small corrections.

The phase factor,  $\theta$ , in the hopping terms introduces a phase twist along the ring. Equivalently, it represents a magnetic field of  $\theta/2\pi$  flux quantum that threads through the ring. It plays a role similar to the role of the momentum in a translation invariant crystal, and is required in order for the Chern number to be defined.

For an integer  $\theta/2\pi$  this phase factor can be gauged out. Hence, the spectrum and the topological properties are periodic in  $\theta$  modulus  $2\pi$ . Moreover, since  $\theta$  appears in the Hamiltonian only via  $\theta/L$ -terms, perturbation theory shows that its influence on the spectrum is suppressed by a factor of  $1/L$ . Therefore, for large enough  $L$  the gaps of  $H_b$  are well defined for every  $\theta$ .

We can therefore summarize that a gap of  $H_b$  which remains open for every  $\theta$  and for increasing  $L$ , corresponds one-to-one to a gap of the AA model. Consequently, such a gap with a non-trivial Chern number has the same physical properties in both models in the thermodynamic limit.

A convenient way to evaluate the Chern number associated with a given gap is to consider the spectral projector on the states below this gap

$$P(\phi, \theta) = \sum_{E_n < E_{gap}} |n\rangle\langle n|, \quad (4)$$

where  $|n\rangle$  is an eigenstate of the system with energy  $E_n$ , and  $E_{gap}$  is the energy at the center of the gap.

For  $\epsilon = 2\pi l/L$  and  $l = 0, 1, \dots, L-1$  there is always some  $n_\epsilon \in \{0, 1, \dots, L-1\}$  such that  $\cos(2\pi\bar{b}_L n + \phi + \epsilon) = \cos(2\pi\bar{b}_L(n + n_\epsilon) + \phi)$ , independent of  $\phi$ . For a prime  $L$

it is also guaranteed that there is an  $n_\epsilon$  for the minimal  $\epsilon = 2\pi/L$ . If we denote a translation operator of  $n_\epsilon$  sites by  $\hat{T}_\epsilon$ , then  $H_b(\phi + \epsilon) = T_\epsilon H_b(\phi) T_\epsilon^{-1}$ , and accordingly  $P(\phi + \epsilon) = T_\epsilon P(\phi) T_\epsilon^{-1}$ . The equivalence between the phase and spatial shifts implies that the shifts have no physical consequences, such as closing the energy gaps. In the thermodynamic limit  $\epsilon$  becomes continuous, which means that the spectrum is independent of  $\phi$ . For finite but large enough  $L$  the spectrum depends on  $L$ , but the gap structure does not. Therefore  $P(\phi)$  is a well defined quantity. Note that by definition

$$\begin{aligned} \partial_\phi P(\phi + \epsilon) &= \lim_{\Delta \rightarrow 0} \frac{1}{\Delta} (P(\phi + \epsilon + \Delta) - P(\phi + \epsilon)) \\ &= \lim_{\Delta \rightarrow 0} T_\epsilon \frac{1}{\Delta} (P(\phi + \Delta) - P(\phi)) T_\epsilon^{-1} \\ &= T_\epsilon \partial_\phi P(\phi) T_\epsilon^{-1}. \end{aligned} \quad (5)$$

The Chern number associated with the gap is given by

$$\nu = \frac{1}{2\pi i} \int_0^{2\pi} d\phi d\theta C(\theta, \phi), \quad (6)$$

where

$$C(\phi, \theta) = \text{Tr} \left( \left[ P, \left[ \frac{\partial P}{\partial \phi}, \frac{\partial P}{\partial \theta} \right] \right] \right), \quad (7)$$

is the Chern density. Therefore,

$$\begin{aligned} C(\phi + \epsilon) &= \text{Tr} ([P(\phi + \epsilon), [\partial_\phi P(\phi + \epsilon), \partial_\theta P(\phi + \epsilon)]) \\ &= \text{Tr} (T_\epsilon [P(\phi), [\partial_\phi P(\phi), \partial_\theta P(\phi)]] T_\epsilon^{-1}) \\ &= C(\phi). \end{aligned} \quad (8)$$

We can see that  $C(\phi)$  is periodic with  $1/L$  periodicity, which means that

$$\begin{aligned} \int_0^{2\pi} d\phi C(\phi) &= L \int_0^{2\pi/L} d\phi C(\phi) \\ &= 2\pi C(\phi = 0) + O(1/L). \end{aligned} \quad (9)$$

Since the Chern density,  $C$ , is independent of  $\phi$  in the thermodynamic limit, the Chern number  $\nu$  can be attributed to any Hamiltonian  $H(\phi)$  for any given  $\phi$ .

The generalization of this proof to other QCs is straightforward, since it relies only on the periodicity of the Hamiltonian in  $\phi$  and on the equivalence between phase shifts and translations. Given a Hamiltonian of a  $D$ -dimensional QC with  $d$  quasi-periodic terms, which can be associated with phase shifts, one can define a periodic version of the Hamiltonian (similar to  $H_b$ ). The same insensitivity to the periodicity and phase twists in the thermodynamic limit still holds, as well as the conversion from phase shifts to translations. Therefore any gap of such a  $D$ -dimensional Hamiltonian is characterized by the topological classification of a Hamiltonian of  $D + d$  dimensions.

## II. THE ADDITIONAL DEGREES OF FREEDOM OF “CUT AND PROJECT” QUASICRYSTALS

In the main body of the paper we considered two examples of 1D quasicrystals that exhibit topological properties: (i) the “diagonal” Aubry-Andre model [cf. equation (1)] in which the quasi-periodicity is in the on-site potential, and (ii) its “off-diagonal” version [cf. equation (2)] that has its quasi-periodicity in the hopping term. We then argued that tight-binding Hamiltonians of other QCs and of higher dimensions also have such topological properties.

However, there is a class of QCs that is obtained by a “cut and project” method<sup>14</sup>, for which one might think that our argument does not hold. For these QCs the additional d.o.f. are shifts of the “cut” in the higher-dimensional space. Such shifts modify the Hamiltonian in a discontinuous manner. Hence, as our argument relied on the continuity of the on-site and hopping terms as a function of the additional d.o.f., it seems that these QCs do not fit our framework.

We now show that our generalization indeed includes such QCs. This is done by defining a smooth version of the projection procedure. This procedure keeps the energy gaps unchanged, and therefore has the same topological properties. For example, in 1D, a QC can be obtained by projecting a square lattice on the line  $y = x/\tau$ , where  $\tau$  is irrational. The normalized spacings between the lattice sites  $n$  and  $n + 1$  is therefore

$$d_n = 1 + (\tau - 1) (\lfloor (n + 2) / \tau \rfloor - \lfloor (n + 1) / \tau \rfloor). \quad (10)$$

The case of  $\tau = (1 + \sqrt{5}) / 2$  is the well studied Fibonacci QC<sup>14</sup>. For  $\tau > 1$  a smoothed projection can be of the form

$$\bar{d}_n(\beta, \phi) = 1 + \frac{\tau - 1}{2} \times \left( 1 - \tanh \beta \left[ \sin \left( 2\pi \left[ \frac{2n + 3}{2\tau} - \frac{1}{4} \right] + \phi \right) + \cos \frac{\pi}{\tau} \right] \right). \quad (11)$$

It can be easily shown that  $\lim_{\beta \rightarrow \infty} \bar{d}_n(\beta, \phi = 0) = d_n$ . Note that  $\phi$  is embedded into  $\bar{d}_n$ , in a way that is consistent with our general argument.

The spacing between the lattice sites enters the Hamiltonian through the hopping terms. Since a Hamiltonian with  $\bar{d}_n$  can be continuously deformed into one with  $d_n$  without closing the energy gaps, they belong to the same topological class. Therefore, given a QC which is obtained by a “cut and project” procedure, one should find a smoothed version of the projection and accordingly obtain a smoothed Hamiltonian. Now, the topological properties of the “cut” Hamiltonian can be deduced from the smoothed one. Note, that for “cut and project” quasi-periodicity which is incorporated in the on-site terms, a similar smoothing can be performed. Thus, we have shown that the “cut and project” QCs also fit into our general argument.